CFD ANALYSIS OF A TURBULENT JET BEHAVIOR INDUCED BY A STEAM JET DISCHARGE THROUGH A SINGLE HOLE IN A SUBCOOLED WATER POOL

Hyung Seok Kang, Young-June Youn and Chul-Hwa Song

Korea Atomic Energy Research Institute, Korea
Daedeok-daero 1045, Yuseong-gu, Daejeon, 305-353, Korea

Abstract
A Computational Fluid Dynamics (CFD) analysis for a turbulent jet flow induced by a steam jet dischareged into a subcooled water pool was performed for 10 seconds of transients to investigate whether currently available CFD codes can be used suitably as a tool to validate the development of the correlations for a turbulent jet and to analyze thermal-hydraulic behavior in a condensation pool for an advanced reactor. As for the numerical experiment, a sensitivity calculation was conducted to elucidate factors which can produce different CFD results by varying mesh distribution, numerical model for a convection term and the turbulent models. The velocity and the temperature difference of in a region between the sparger and the pool wall has not been observed in the sensitivity calculation. The comparison of the CFD results with test data shows that the CFD analysis does not accurately simulate the local phenomenon of a turbulent jet existing downstream of a steam jet.

1. INTRODUCTION

The experimental and CFD research for an unstable steam condensation in a DCC (Direct Contact Condensation) which may happen in the IRWST (In-containment Refueling Water Storage Tank) of APR1400 (Advanced Power Reactor 1400 MWe) were performed to understand the phenomenon of a DCC (Kim et al, 1997; Song et al., 2007). One of the main reasons for the unstable steam condensation was found to be an increased temperature of a turbulent water jet entraining on a steam jet (Su, 1981). Thus, a thermal mixing test by discharging steam through a sparger into a subcooled water was recently performed to investigate a local temperature of the pool water around the sparger (Park et al., 2005 & 2007). The CFD analysis using so-called the condensation region model for the thermal mixing test was conducted to develop a methodology which can be applied to the safety assessment of the IRWST (Kang et al., 2007; Kang & Song, 2008). This analysis shows that a commercial CFD code with the condensation region model can be used to analyze overall pool behaviour if a sufficiently fine mesh distribution and a proper numerical model are adopted to use.

The thermal-hydraulic load onto the IRWST wall was also evaluated for each discharging phase of water, air and steam through the sparger (Park et al., 2005 and Ra, 1999). In the dynamic load analysis of the steam discharge phase, the maximum velocity, temperature and the width of the turbulent water jet induced by the steam condensation were used as the input data (Ra, 1999). It seems to be very useful for the evaluation of a thermal-hydraulic load if an empirical correlation to accurately predict the velocity and temperature of a turbulent water jet is developed. Therefore, a fundamental test to measure the velocity and temperature distribution of a turbulent jet during the steam discharging through a single-hole sparger into a subcooled water pool was performed to develop the correlations (Kang et al., 2008). However, the velocity and temperature was not measured at the upstream region of the turbulent jet existing downstream of a steam jet because a measurement device might disturb the turbulent jet behaviour. Also, a far-away region from the turbulent jet was also not measured since we could not ensure a quasi-steady state behaviour of pool during the steam discharge.

A commercial code, the CFX-11 (ANSYS, 2007) was introduced in this study to assist the development of the correlations to accurately predict the velocity and temperature of a turbulent water jet based on the validation work of the CFX-11 against the measured data near the steam jet region. It would also be very helpful for understanding the effect of a steam jet condensation on the turbulent jet to compare the measurements of the velocity and temperature distribution with those data predicted by a theory for the turbulent jet of a single phase (Abramovich, 1963).

2. THE TURBULENT JET SOLUTION BY A THEORY

The solution from a turbulent jet theory regarding the velocity and temperature distribution can be meaningfully used as the reference data for a comparison of measurements and CFD results. The theory of the Tollmien's axially symmetric source (Abramovich, 1963) has been mainly applied to a submerged turbulent flow which seems to be similar to the turbulent flow induced by the steam condensation in the subcooled water pool. This theory assumes that the turbulent jet flow starts from the point source and some of the axial flow moves upward due to the turbulent shear stress as the turbulent jet propagates. The similarity method (Table 1) was introduced to solve the Tollmien's model, and the obtained solutions of the flow field and heat transfer can be presented in dimensionless forms, as shown in Fig. 1, depending on the coefficient of "a" related to a mixing length model (Abramovich, 1963 and Chung, 2005).

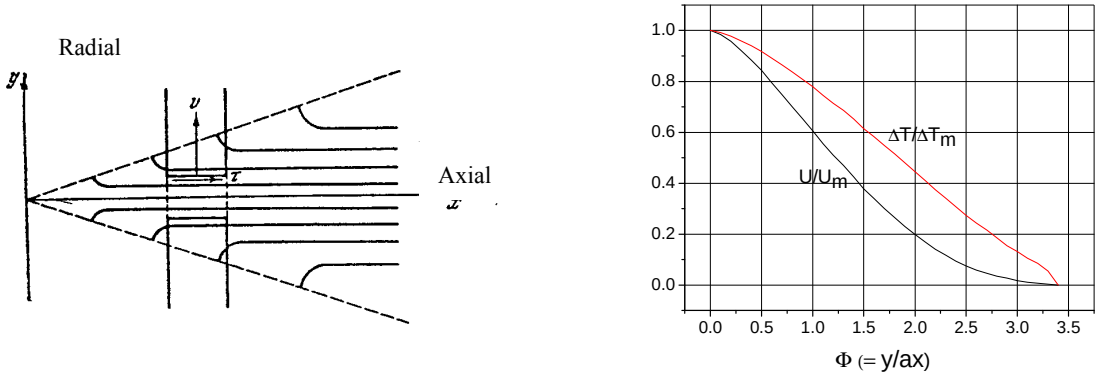

(a) Axially Symmetric Turbulent (b) Similarity Solution (dimensionless)

Fig. 1: Axi-Symmetric Turbulent Source' Solution (Abramovich, 1963)

Table 1: Similarity Method for the Tollmien's Theory (Abramovich, 1963)

Flow Field	Heat Transfer
$\frac{U}{U_m}=f\left(\frac{y}{x}\right)=f(\eta)$	$\frac{\Delta T}{\Delta T_m}=\theta\left(\frac{y}{x}\right)=\theta(\eta)$
$U=\frac{m}{x}\frac{F'(\eta)}{\eta}$, $V=\frac{m}{x}\left[F'(\eta)-\frac{F(\eta)}{\eta}\right]$	$\Delta T=\Delta T_m\theta(\eta)=\frac{k}{x}\theta(\eta)$
$UV+\frac{1}{y}\frac{\partial}{\partial x}\int_{\infty}^{y}U^2 y dy+c^2x^2\left(\frac{\partial U}{\partial y}\right)=0$	$\Delta TV+\frac{\partial}{\partial x}\int_{\infty}^{y}\Delta TU dy+c^2x^2\frac{\partial U}{\partial y}\frac{\partial T}{\partial y}=0$
$\left[F''(\varphi)-\frac{1}{\varphi}F'(\varphi)\right]^2=F(\varphi)F'(\varphi)$	$c^2\theta'(\eta)\left[F''(\eta)-\frac{F'(\eta)}{\eta}\right]=F(\eta)\theta(\eta)$
$\varphi=\frac{y}{ax}$, $a=\sqrt[3]{c^2}$, $\frac{U_m}{U_o}=\frac{0.96}{\frac{ax}{R_o}}$	$\frac{\Delta T}{\Delta T_m}=\theta(\eta)=\sqrt{\frac{F'(\eta)}{\eta}}=\sqrt{\frac{U}{U_m}}$

3. EXPERIMENT OF THE TURBULENT JET

3.1 Experimental Facility

The GIRLS facility with a single-hole sparger (Fig. 2) submerged in a subcooled water tank was used for the experiment of the turbulent jet induced by the steam condensation (Song et al., 2007; Choi et al., 2007). The diameter of the single hole on the surface of the sparger is 1 cm. Steam generated in the

steam boiler is provided along a pipe from the boiler to the single-hole sparger. During this delivery, the temperature, pressure and mass flow rate of the steam were measured, and the measured temperature and the pressure inside the sparger provide the information on the discharged steam. The temperature of the pool water is reported by averaging the 6 Thermocouples (TCs) located near the tank wall. In order to measure the velocity and temperature distribution of the turbulent jet without disturbing the shape of the jet flow, a movable spool of pitot tube and TCs was introduced to provide information on velocity and the temperature simultaneously in the axial and radial directions. The geometric information of the measurement spool is shown in detail in Fig. 2.

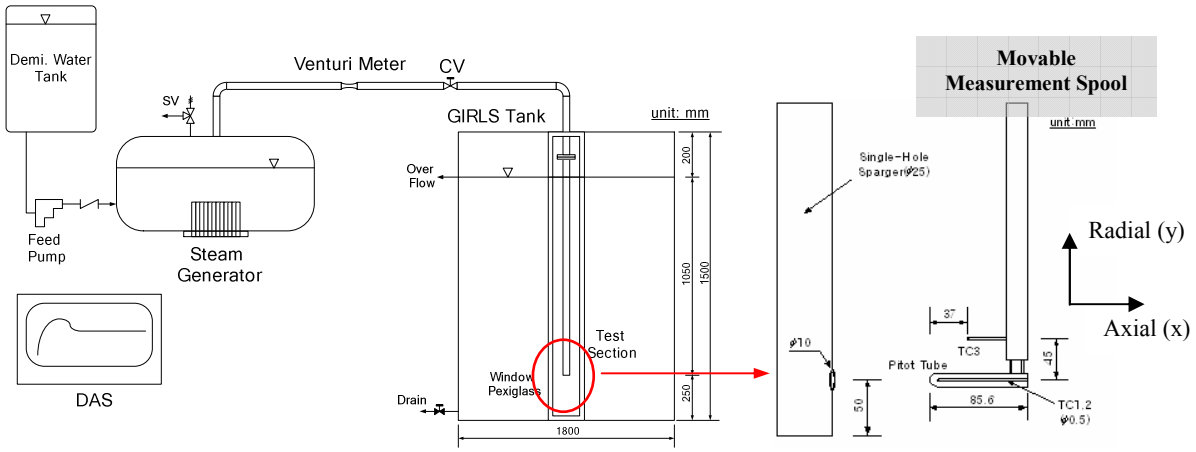

Fig. 2: Schematic Diagram of the GIRLS Facility

3.2 Experimental Matrix

The experiment for the turbulent jet was performed to investigate the stable condensation region under the quasi-steady state by discharging the steam jet of about 1,000 kg/m^{2}s into the lower temperature of the tank water (Kim et al., 2005; Kang et al., 2008). In order to observe the effect of pool water temperature on the turbulent jet, five cases were selected as shown in Table 2. The measurement spool is continually moved to measure the velocity and temperature of the turbulent jet in the radial direction at the same axial location. The axial measurement location is defined as a horizontal distance from the exit of the single hole to the measurement position. The radial measurement location is a vertical distance at the same axial location, and is increased by 0.25cm from the center of the turbulent jet. The total number of measurement locations is 122 points, and the duration of a measurement at one location is about 4 seconds. While moving the measurements spool manually, the temperature of the pool water is increased by 10~20% of the initial temperature due to the energy of the discharge steam jet (Table 2). The uncertainty of the measurement devices is shown in Table 3.

Table 2: Experimental Matrix

	Temp. of Tank Water (℃)	Mass Flux (kg/m^{2}s) & Temp. of Steam (℃)	Axial Measuring Location (cm)	Radial Measuring Location (cm)
Case 1	15.0~22.4	G=999.9±10.2, T_s=165.6±0.6	8, 12, 16	0 ~ 2.25 (△y=0.25)
Case 2	27.4~35.2	G=997.9±11.5, T_s=165.8±0.6	8, 12, 16	0 ~ 2.25 (△y=0.25)
Case 3	31.1~35.6	G=1008.1±24.9, T_s=166.2±1.2	8, 12, 16	0 ~ 1.75 (△y=0.25)
Case 4	36.4~40.6	G=1002.7±29.8, T_s=166.0±1.4	8, 12, 16	0 ~ 1.75 (△y=0.25)
Case 5	38.8~47.6	G=991.3±19.2, T_s=165.7±1.0	8, 12, 16, 20	0 ~ 2.75 (△y=0.25)

Table 3: Information on the Instrumentations

Measurement variable	Number	Uncertainty (%)
Temperature	15	± 0.7
Static pressure	2	± 0.05
Volumetric flow	1	± 1.35
Velocity (Pitot tube)	1	± 2.0

3.3 Experimental Results and Discussion

It is shown in Fig. 3 that the velocity value at the jet centerline is decayed. This is because the width of the jet is increased as the turbulent jet propagates along the axial direction. This flow pattern is very similar to that of the single phase jet. In Fig.3, the velocity values at the axial location of 12cm, 16cm, 20cm were normalized by the values measured at 8cm, and the velocity value from the Tollmien's theory is obtained by the relation of U_m/U_o (Table 1). During the normalization process, the dependency of the coefficient of "a" related to the mixing length model is disappeared. The predicted values by the Tollmien's theory are less than about 10% of those of the test results. When using the theory, the point of the turbulent source was assumed as the center point of a single-hole of the sparger.

In order to elucidate the effect of a steam condensation on the turbulent jet, it is necessary to quantitatively evaluate the spreading value of the jet width by comparing it with the value of a single phase by the Tollmien's theory, because the entrained water from the pool water into the steam jet may increase the jet width of the turbulent jet. It was also observed that the diameter of the vapor core in the steam jet is expanded to 1.63 times that of the single-hole as the steam jet is discharged with an ellipsoidal shape under a steam mass flux of about 1,000 kg/m^{2}s (Kim, 2001). The comparison results for the normalized radial velocity of the test results with the Tollmien's theory at the axial locations of 8cm, 12cm, 16cm, 20cm are shown in Fig. 4. The recommended coefficients for "a" (Table 1) concerning the spread of the single phase jet are 0.066, 0.070 and 0.076 (Abramovich, 1963). From our comparisons, however, the velocity distribution with these values of the a-coefficient does not agree with the test results well as shown in Fig. 4, whereas the theory's solutions predicted well the test results if the coefficient of 0.082 is used instead. This may mean that the extent of the radial spread of the turbulent jet induced by the steam condensation is about 10 ~ 25% larger than that of a single phase jet due to the effect of an entrainment and the expansion phenomena.

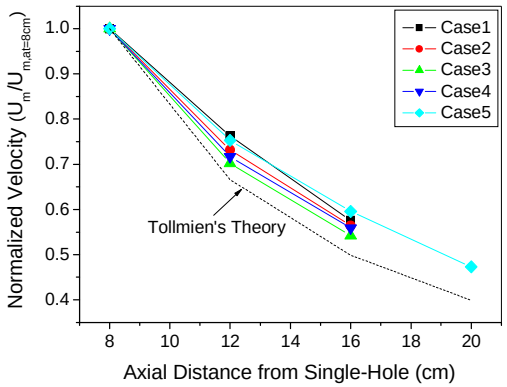

Fig. 3: Comparison of the Measured Velocity at the Centerline with the Tollmien's Theory

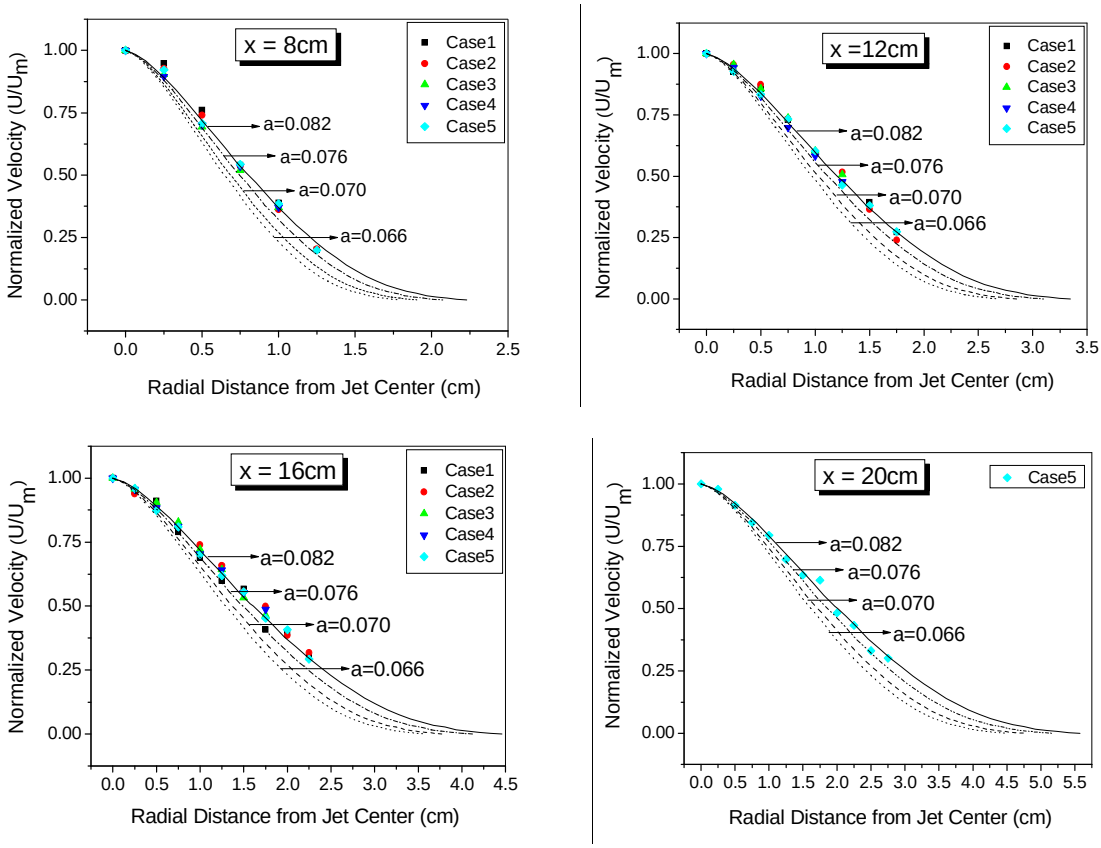

Fig. 4: Comparison of the Measured Velocity in the Radial Direction with the Tollmien's Theory (a=0.066, 0.07, 0.076, 0.082, Φ=y/ax)

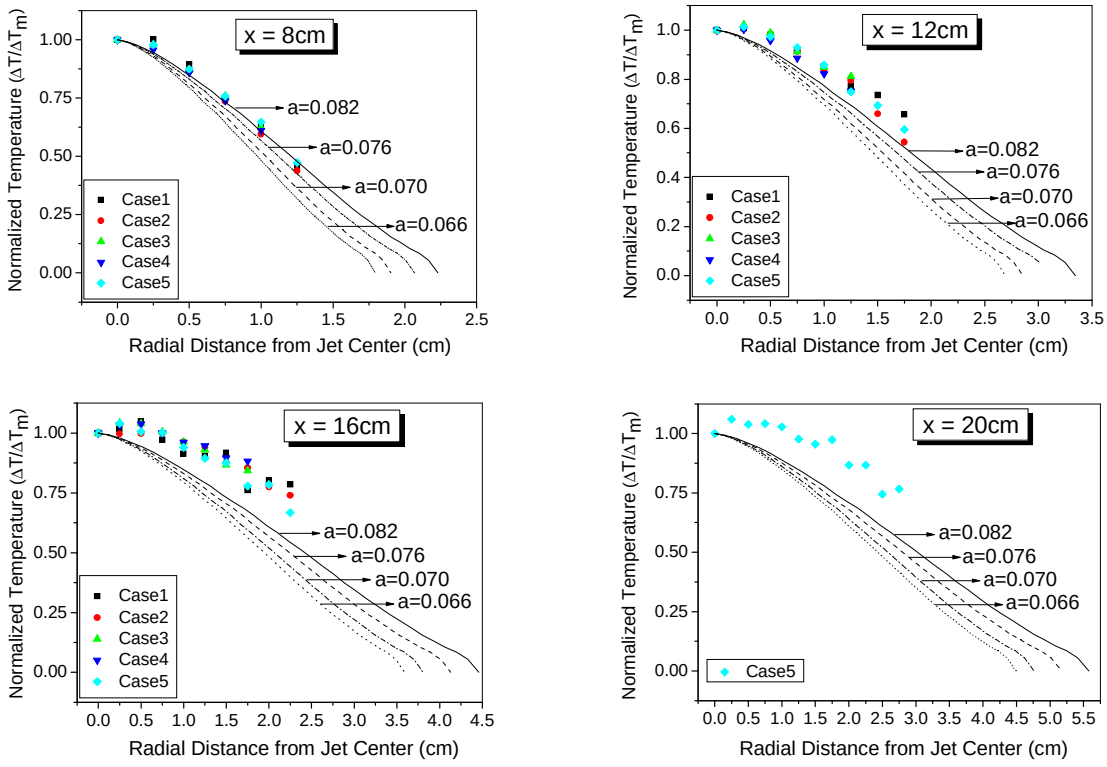

Fig. 5: Comparison of the Measured Temperatures in the Radial Direction with the Tollmien's Theory (Average T_∞ of Case1 ~ Case5 = 15.7℃, 27.8℃, 31.7℃, 36.8℃ and 39.3℃)

The normalized temperature distribution along the radial direction of the test results and Tollmien's theory by varying the coefficient of "a" at the axial locations of 8cm, 12cm, 16cm and 20cm are shown in Fig. 4. At 8cm, the predicted values by the Tollmien's theory with "a = 0.082" agreed well with the test data, but the predicted value by the Tollmien's theory at 12cm, 16cm and 20cm are located lower than the test data. It can be deduced that these differences may be caused by using the increased values of the average pool water temperature (T_∞) which has been used in the normalization process of the test data along the radial direction at the same axial location. In the experiments, the temperature difference, $\triangle T_m (=T_m - T_\infty)$, measured at the centerline is decreased due to an increase of the average T_∞ when compared to the instant temperature of T_∞ measured at the jet centerline. In the case of the local temperature difference of $\triangle T (=T(x,y)-T_\infty)$, a reverse situation happens. This effect is clearly shown in the temperature results at 16cm and 20cm because the temperature difference between the measured data at the radial direction and pool water is smaller than that of 8cm. It is expected that the dimensionless temperature distributions at 12cm, 16cm and 20cm agree well with those values by the Tollmien's theory when using a constant value for a pool water temperature, because the comparison of the velocity results at those axial locations shows a good agreement.

When using the Tollmien's theory with the value of 0.082 for the coefficient of "a", the velocity and the temperature distribution of the turbulent jet in the radial direction along the axial location can be obtained. However, the maximum velocity (U_m) along the centerline of the turbulent jet by the Tollmien's theory can not be obtained because of the steam condensation phenomenon. In this region, the condensed water velocity at the downstream part is less than 5% that of the steam velocity at the upstream part, because the water density is about 1,000 times larger than that of the steam. Therefore, a correlation to predict the maximum velocity at a jet centerline is proposed like as Eq. (1) with the help of a previous one and the test data (Tin, 1983; Choi et al., 2007). The error of this correlation is less than ±10%.

In Eq. (1), "y_c" is the characteristic length in the radial direction from the centerline to the location at 50% of the U_m. In general, y_c is dependent on the axial distance from the jet discharge nozzle in a single phase jet, whereas y_c of the turbulent jet induced by a steam condensation may vary depending on the condition of the steam properties and the pool water temperature. Thus, a new variable of "x-L" of which the physical meaning is the length from the end of the steam jet penetration length (L) (Kim, 2001) to the measured location along the axial location is introduced to account for the variation of the mass flux of the steam jet and the temperature of the tank water. The correlation for the y_c (Eq. (2)) using the new variable was developed with an error of ±10% based on the test results (Kang et al., 2008) And a correlation for the maximum temperature (Eq. (3)) at the jet centerline, based simply on the test results, was also proposed and the error of this correlation was about ±20%.

$$U_m = 0.95 \frac{dU_o}{y_c} \sqrt{\frac{\rho_v}{\rho_l}} \tag{1}$$

$$y_c = 0.11(x-L) + 0.3d \tag{2}$$

$$\frac{T_m(x-L)}{T_\infty} = e^{-y_c}\left[0.36(x-L) + 1.8d\right] \tag{3}$$

The correlations for the velocity and the temperature of the turbulent jet at the centerline were developed based on our measured data at the axial locations of only 8~20cm from the exit of the steam discharge hole. To use these correlations at other regions, a supplementary test should be performed, and the correlations should be validated against the test results. However, if the pitot tube-TC spool moves closer to the throat of a discharging hole to measure the velocity and temperature, the turbulent jet may be disturbed. Therefore, the CFD method was introduced in this study to help the validation work for the extension of the applicable range of the correlations of turbulent jet.

4. CFD ANALYSIS

4.1 Modelling Strategy and Grid Model

CFD codes can be used as tools to assist the development of the correlations to predict the velocity and temperature of a turbulent water jet produced by condensing steam jet discharged into a water pool. The test case selected for the CFD validation is the case-3 in Table 2. First of all, the local velocity distributions at the axial location of 8 ~ 12cm were carefully compared with the test results before the temperature comparison and the Tollmien's theory with a coefficient of "a = 0.082" because the heat transfer enhancement due to the turbulence effect is calculated based on the velocity results by the Reynolds analogy concept implemented in the CFX-11. According to the previous CFD analysis results (Kang & Song, 2008) and the best practice guidelines (OECD/NEA, 2007), it was observed that the prediction of turbulent jet behaviour in the subcooled water pool is mainly dependent on the mesh distribution, the discretization method of the convection term and the turbulent model. Therefore, a sensitivity calculation by considering these factors has been performed to evaluate the uncertainty of CFD analysis results.

The CFD analysis for the turbulent jet considered in our experiments has to be made as a transient state because a local thermal mixing pattern of the pool water is proportional to the discharged time of a steam jet. However, it is difficult to simulate a whole steam discharging time in the test, and the local velocity and temperature behaviour at 8 ~ 16cm may be less dependent on the steam discharging time. A transient calculation of 10 seconds with a time step of 0.001 second has been performed. A denser cells distribution inside the jet boundary is usually recommended to obtain a well converged solution of the jet flow in a CFD analysis (Kang & Song, 2008; Yoon & Park, 2007). Therefore, the axi-symmetric grid model with a fine mesh distribution (Fig. 6) was introduced because the turbulent jet behaviour may be axi-symmetric with regard to the center of the single-hole, and this model can save the computational time. In the grid model, the flow region (Fig. 6 "B") from the single-hole to the axial location of 8cm with a diameter of 4cm in the radial direction inside the steam and turbulent jet boundary has been excluded from the computational domain to start the CFD calculation from the turbulent jet at the 8 cm, and instead the inlet condition is provided from the test data and the Tollmien's theory at 8cm. The purpose of this modeling is first to evaluate the CFD results against the test results at the axial locations from 8 to 16cm before applying the CFD calculation into other regions in the whole region of water pool. In order to evaluate the uncertainty of CFD results due to the mesh distribution, the sensitivity calculation was set up as in Table 4 including a numerical model of the convection term, a turbulent model and an entrainment model (Kang & Song, 2008).

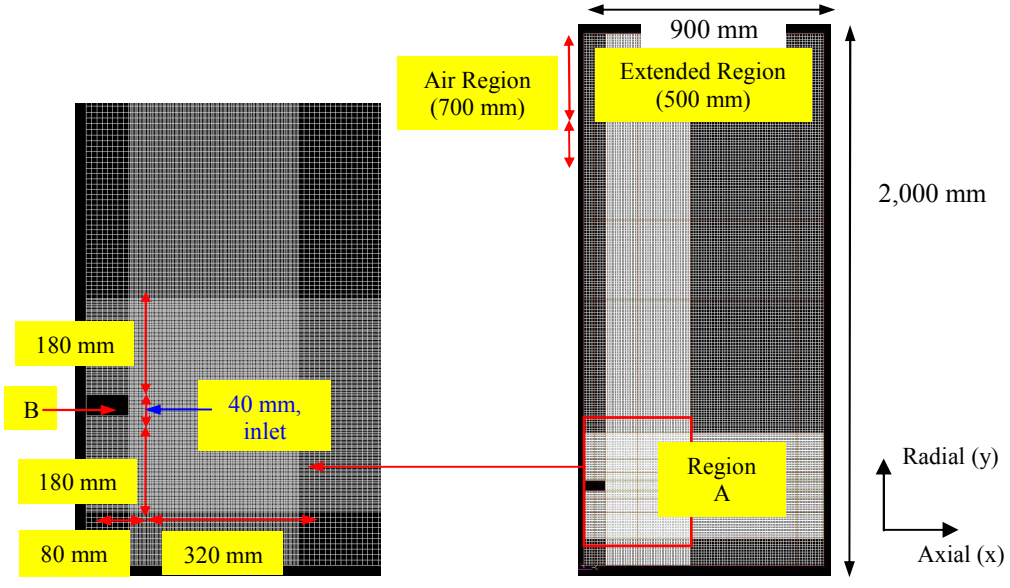

Fig. 6: Axis-Symmetric Grid Model

Table 4: CFD Sensitivity Calculation Conditions

	Cell Dimension In Region A	Total Number of Cells	Convection Term Discretization	Turbulent Model	Entrainment Model (Kang & Song, 2008)
Case-1	△x = △y = 2.5 mm / cell	59,392	High Resolution	SST	No
Case-2	△x = △y = 5.0 mm / cell	29,216	High Resolution	SST	No
Case-3	△x = △y = 2.5 mm / cell	59,392	Upwind	SST	No
Case-4	△x = △y = 2.5 mm / cell	59,392	High Resolution	k-ε	No
Case-5	△x = △y = 2.5 mm / cell	59,392	High Resolution	SST	Yes
● Standard wall function was used for all Cases. ● Except region A, other region is △x = △y = 10.0 mm / cell or △x =10.0, △y = 2.5 (5.0) mm / cell					

4.2 Boundary Conditions and Governing Equations

The inlet boundary condition (ANSYS, 2007), the Dirichlet condition, was set at the axial location of 8cm with a length of 4cm in the radial direction (Fig. 6) with the velocity and temperature distribution as shown in Fig. 7. The values of the turbulent properties at the inlet were set as 10% of intensity because the eddy motions are very actively generated when the steam jet is discharged through holes. The pressure outlet boundary condition (ANSYS, 2007), the Neumann condition, was set for the pool upper region, which only allows an outflow of air. A symmetry condition was applied to the center of the sparger.

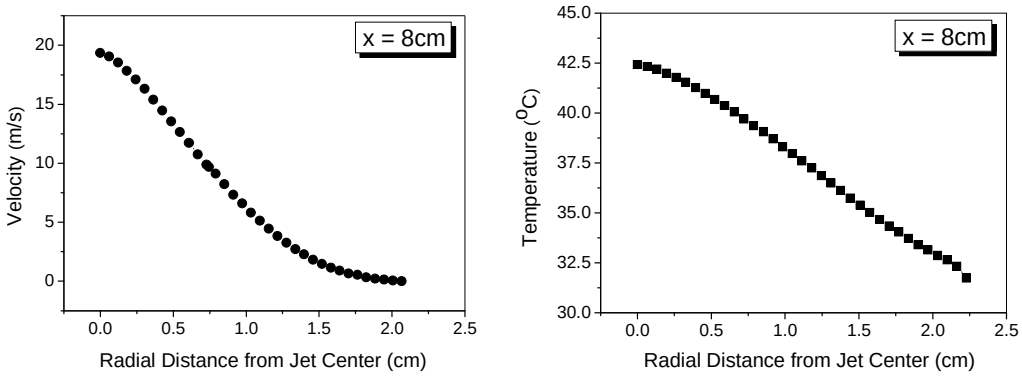

Fig. 7: Inlet Boundary Conditions

Thermal mixing phenomenon in the subcooled water pool was treated as an incompressible flow, a free air surface over the pool water, a turbulent flow, and a buoyancy flow. Therefore, the governing equations used in this study are the Navier-Stokes and energy equations with a homogenous multi-fluid model under a coupled algorithm (ANSYS, 2007). The turbulent flow is simulated by the standard k-ε turbulent model (Eq. (4)~(6)) and the shear stress transport (Eq. (7)~(9)), and the buoyancy is modelled by the Boussinesq approximation. As for the numerical model for the convection term, the first-order upwind (β=0 in Eq. (10)) and the high resolution model are used (β=1 in Eq. (10)). In the homogenous model, the inter-phase mass and heat transfer is neglected. Each transport quantity in the governing equations except for the volume fraction is summed over all the phases to provide a single transport quantity. As a calculation method, 10 iterations are performed with a time step of 0.001 seconds until the mass, enthalpy, and velocity residual of the water reach below a value of 1.0E-04, except for the enthalpy of the Case-2.

$$\frac{\partial k}{\partial t}+U_j\frac{\partial k}{\partial x_j}=P_k-\varepsilon+\frac{\partial}{\partial x_j}\left[\left(\nu+\frac{\nu_t}{\sigma_k}\right)\frac{\partial k}{\partial x_j}\right] \tag{4}$$

$$\frac{\partial \varepsilon}{\partial t}+U_j\frac{\partial \varepsilon}{\partial x_j}=C_{\varepsilon 1}\frac{\varepsilon}{k}P_k-C_{\varepsilon 2}\frac{\varepsilon^2}{k}+\frac{\partial}{\partial x_j}\left[\left(\nu+\frac{\nu_t}{\sigma_\varepsilon}\right)\frac{\partial \varepsilon}{\partial x_j}\right] \tag{5}$$

$$\nu_t = C_\mu \frac{k^2}{\varepsilon} \tag{6}$$

$$\frac{\partial(\rho k)}{\partial t} + \frac{\partial}{\partial x_i}(\rho U_i k) = P_k - \beta' \rho k\omega + \frac{\partial}{\partial x_i}\left[\left(\mu + \sigma_\omega \mu_t \frac{\partial k}{\partial x_i}\right)\right] \tag{7}$$

$$\frac{\partial(\rho\omega)}{\partial t} + \frac{\partial}{\partial x_i}(\rho U_i \omega) = \alpha\rho S^2 - \beta\rho\omega^2 + \frac{\partial}{\partial x_i}\left[\left(\mu + \sigma_\omega \mu_t \frac{\partial \omega}{\partial x_i}\right)\right] + 2(1-F_1)\rho\sigma_{\omega 2}\frac{1}{\omega}\frac{\partial k}{\partial x_i}\frac{\partial \omega}{\partial x_i} \tag{8}$$

$$\nu_t = \frac{a_1 k}{\max(a_1\omega, SF_2)} \tag{9}$$

$$\phi_{ip} = \phi_{up} + \beta \nabla\phi \bullet \Delta\vec{r} \tag{10}$$

4.3 Discussion on the CFD Results

The time dependency of the CFD results should be checked before comparing the CFD results of the transient state with the test results of the quasi-steady state. The velocity, temperature and the normalized velocity distribution in the radial and axial directions of the Case-1 at 7sec, 8sec, 9sec and 10sec are shown in Fig. 8. From the CFD results shown in Fig. 8, it is observed that the local phenomena at the region between the inlet and the pool wall do not depend on the simulation time except the average temperature of the pool water. And the turbulent jet discharged from the inlet propagates until a half length of the radius of the pool and then slightly moved upward due to a buoyancy force and the circulation flow developed at the bottom region. The comparison of the normalized velocity distribution along the radial direction at the axial locations of 12cm and 16cm also shows that the time dependency could be neglected. Therefore, the CFD results at 10 seconds have been selected for the comparison with the test results.

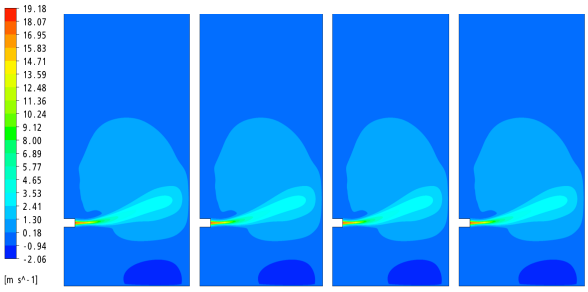

7 sec. 8 sec. 9 sec. 10 sec.

(a) Velocity Distribution Contour

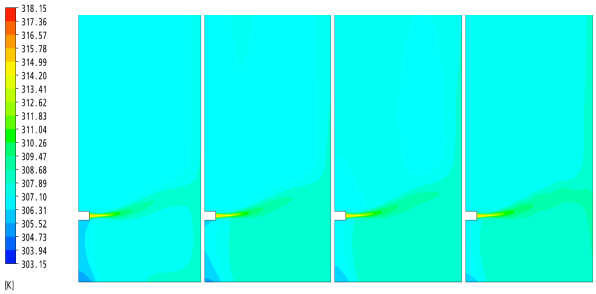

7 sec. 8 sec. 9 sec. 10 sec.

(b) Temperature Distribution Contour

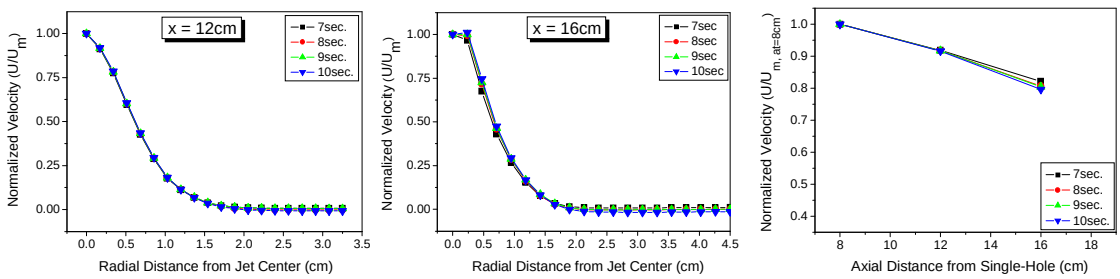

(c) Normalized Velocity Distribution at the 12cm, 16cm and Jet Centerline

Fig. 8: Velocity, Temperature and Velocity Distribution of the Case-1 at 7, 8, 9 and 10 sec.

The CFD sensitivity results show that the velocity difference in the radial direction (Fig. 9 (a)) due to the mesh distribution, the numerical model for the convection term and the turbulent model is less than 5%. This may come from the fact that the location for the comparison of the CFD results is the region at the front of the tank wall where the flow direction has not changed yet due to a collision effect. However, a velocity difference of 30 ~ 40% has been found when comparing the CFD results with the test results at the same location (Fig. 9 (a)). This may be caused by the circulation flow developed around the turbulent jet (Fig. 10, A) which reduces the momentum diffusion in the radial direction, and also the lower velocity parts at the top (Fig. 10, B) and the bottom (Fig. 9, C) on the inlet region are moved to a higher velocity part at the center region (Fig. 9, D). This over-predicted circulation flow is also found in the result for the Case-5.

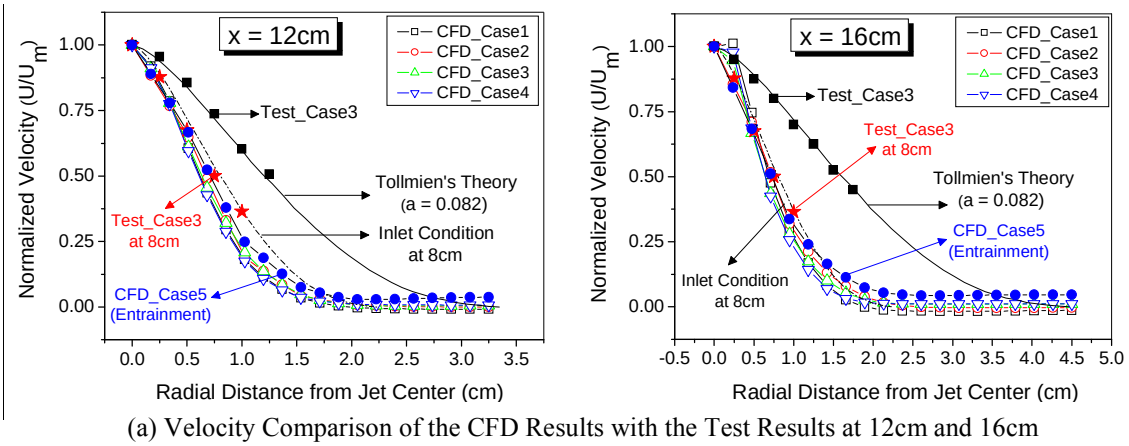

(a) Velocity Comparison of the CFD Results with the Test Results at 12cm and 16cm

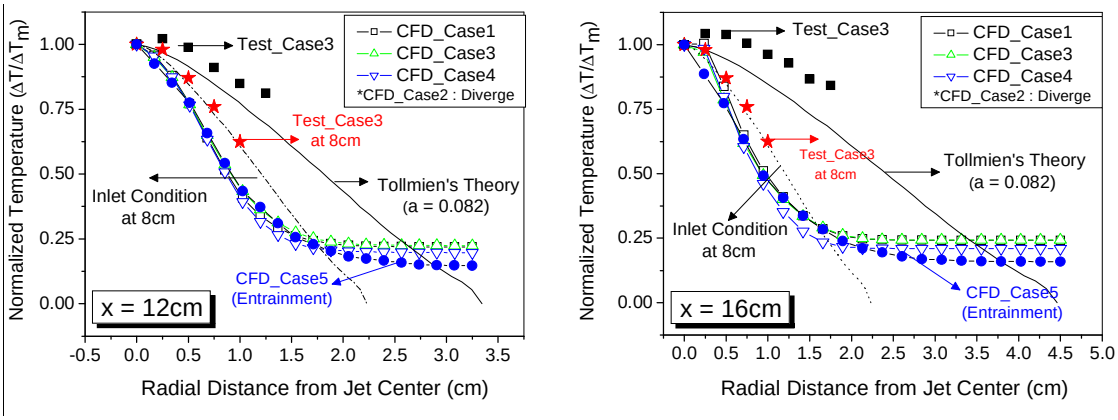

(b) Temperature Comparison of the CFD Results with the Test Results at 12cm and 16cm

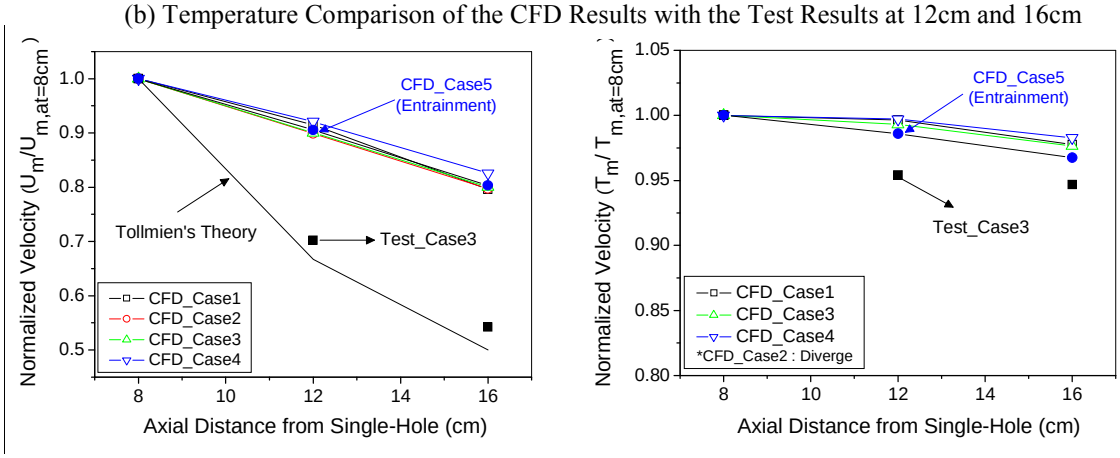

(c) Velocity and Temp. Comparison of the CFD Results with the Test Results at Jet Centerline

Fig. 9: Comparison of the CFD results with the Test Results

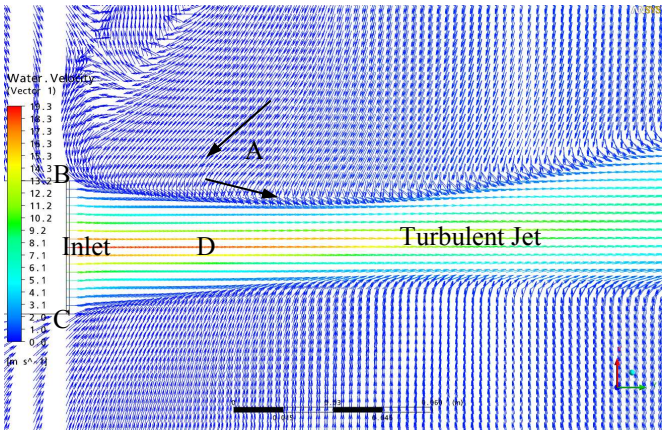

Fig. 10: Velocity Profile around the Turbulent Jet

According to the comparison of temperature (Fig. 9 (b)), the CFD results also do not predict the test data well because the turbulent temperature field is calculated from the velocity results by using the turbulent Prandtl number (ANSYS, 2007). In regards to the curve shape (Fig. 9 (a) and (b)), the curve shape of the temperature results is almost similar to the velocity results in the CFD analysis, whereas the temperature shapes of the Tollmien's theory (Fig. 1, (b)) is different from that of the velocity due to the effect of the square root (Table 1). It is concluded that a careful investigation is necessary to find the reason for this difference. The velocity and temperature along the jet centerline in the CFD results are slowly decayed when compared with the test results. This may also be caused by the reduced transfer of the momentum and energy due to the over-predicted circulation flow in the radial direction which may give rise to a slow decay of the momentum and energy along the axial direction.

5. CONCLUSION AND FURTHER WORK

When a condensing the steam jet is discharged into a subcooled water pool to form a turbulent jet, the macroscopic behaviors of the turbulent jet such as local velocity and temperature distribution is very important. In this study, a CFD analysis of the turbulent jet behavior was investigated to develop the relevant correlations based on its comparison with experimental data. Since the measured range of the velocity and temperature was limited for some practical reasons, the CFD analysis was used to generate the velocity and temperature data at the unmeasured region. As for the first step toward the prediction of overall flow circulation behavior in a condensing pool, the validation work using a commercial code, CFX-11, including the sensitivity analysis was performed against the test results. The sensitivity results of the CFD analysis show that a small difference is observed in the CFD analysis due to a simple flow structure, whereas a large difference between the CFD results and the test results led wrongly predicted location and magnitude of flow circulation, which may reduce the moment and energy transfer in the radial direction and also may slow down the decay in the axial direction. For investigating thoroughly this kind of discrepancies between the analysis and tests, new efforts of experiment and CFD analysis have been recently made for the circulation phenomena to be occurred due to the steam discharge in a subcooled water pool in KAERI.

ACKNOWLEDGEMENTS

This work has been financially supported for the nuclear R&D program from the Korean Ministry of Education, Science and Technology (MEST).

NOMENCLATURE

U_m : maximum velocity at the jet centreline [m/s]
U_o : steam velocity at the exit of steam nozzle [m/s]
$\triangle T_m$: temperature difference of steam and jet at the centreline ($=T_m-T_\infty$)

$\triangle T$: temperature difference of steam and jet at the arbitrary location (=$T(x,y)-T_\infty$)
T_∞ : temperature of the tank water [□]
d : diameter of the single-hole on the sparger [cm]
y_c : radial characteristic length from the centreline to the location of $0.5U_m$ [cm]
L : steam penetration length [cm]

Subscript
l : fluid
v : steam
∞ : ambient state in the subcooled water

REFERENCES

ANSYS Inc., *CFX-11 Manual* (2007)

C.K. Park et al., "Steam Condensation Test Program and Analysis of Hydraulic Loads", Technical Report, Korea Atomic Energy Research Institute, KAERI/TR-2946/2005 (2005).

C.K. Park et al., "Experimental Investigation of the Steam Condensation Phenomena due to a Multi-hole Sparger", Journal of Nuclear Science and Technology, Vol. 44, No. 4, 548-557 (2007).

C. Yoon, J. H. Park, "Simulation of the Internal Flows of an Inlet Diffuser Assembly for the CANDU-6 Moderator Analysis", *Nuclear Technology*, Vol. 160, No. 3, 314-324 (2007).

C.H. Song et al., "Thermal-Hydraulic Tests and Analyses for the APR1400 Development and Licensing", *Nuclear Engineering and Technology*, Vol. 39, No. 4, 299-312 (2007).

G.N. Abramovich, The Theory of Turbulent Jets, pp. 76-85, MIT Press, Boston, U.S. (1963).

G.D. Tin et al., "Thermal and Fluid-dynamic Features of Vapor Condensing Jets", *Heat and Technology*, Vol. 1, No. 1, 13-35 (1983).

H.S. Kang et al., "CFD Analysis for a Thermal Mixing Test by CFX-10 Using a Parallel Computation Technique", *KNS Spring Meeting*, Jeju, Korea, May 10-11 (2007).

H.S. Kang and C.H. Song, "CFD Analysis for Thermal Mixing in a Subcooled Water Tank under a High Steam Mass Flux Discharge Condition", *Nuclear Engineering and Design*, Vol. 238, Issue 3, 492-501 (2008)

H. S. Kang et al., "Development of an Empirical Correlation for the Velocity and Temperature at the Centerline of a Turbulent Jet by a Steam Jet Condensation", *KNS Spring Meeting*, KyungJu, Korea, May 28-30 (2008) (to be published).

H.Y. Kim, "A Study on the Characteristics of Direct Contact Condensation of a Steam jet Discharging into a Quenching Tank through a Single Horizontal Pipe", Ph.D Thesis, KAIST, Korea (2001).

M. K. Chung, "Lecture Note of Computational Turbulence Modeling", KAIST, Korea (2005).

N.H. Choi et al., "Experimental Study of a Turbulent Jet Induced by a Steam Jet Condensation through a Hole in a Water Tank", *Proc. KNS Autumn Meeting*, PyeongChang, Korea, October 25-26, pp. 417-418 (2007).

OECD/NEA, "Best Practice Guidelines for the use of CFD in Nuclear Reactor Safety Application", NEA/CSNI/R(2007)5 (2007).

Su, T.M., Suppression pool temperature limits for BWR containments, United States Nuclear Regulatory Commission, NUREG-0783, (1981).

Y.S. Kim et al., "Steam Condensation Induced Thermal Mixing Experimental Using B&C Facility", Technical Report, Korea Atomic Energy Research Institute, KAERI/TR-2933/2005 (2005).

I.S. Ra, "IRWST Thermal Hydraulic Load Analysis Report", Korea Power Engineering Company, N-001-END461-201 (1999).